Western Indian Ocean
JOURNAL OF
Marine Science

Published biannually

Aims and scope: The *Western Indian Ocean Journal of Marine Science* provides an avenue for the wide dissemination of high quality research generated in the Western Indian Ocean (WIO) region, in particular on the sustainable use of coastal and marine resources. This is central to the goal of supporting and promoting sustainable coastal development in the region, as well as contributing to the global base of marine science. The journal publishes original research articles dealing with all aspects of marine science and coastal management. Topics include, but are not limited to: theoretical studies, oceanography, marine biology and ecology, [redacted] between humans and the coastal and marine environment. In addition, *Western Indian Ocean Journal of Marine Science* features state-of-the-art review articles and short communications. The journal will, from time to time, consist of special issues on major events or important thematic issues. Submitted articles are subjected to standard peer-review prior to publication.

Manuscript submissions should be preferably made via the African Journals Online (AJOL) submission platform ([redacted]). Any queries and further editorial correspondence should be sent by e-mail to the Chief Editor, wiojms@fc.ul.pt. Details concerning the preparation [redacted] the editors or publisher.

ISSN 0856-860X

Cover image: Ponta Mazondúe, Inhaca Island, Mozambique (© Jose Paula, 2014)

Adsorption-desorption of chlorpyrifos in soils and sediments from the Rufiji Delta, Tanzania

Haji Mwevura[1]*, Peter Nkedi-Kizza[2], Michael Kishimba[3†], Henrik Kylin[4]

[1] Department of Sciences, State University of Zanzibar, PO Box 146, Zanzibar, Tanzania

[2] Soil and Water Sciences Department, University of Florida, PO Box 110290, Gainesville, FL 32611-0290, USA

[3] Department of Chemistry, University of Dar es Salaam, PO Box 35061, Dar es Salaam, Tanzania

[4] Department of Thematic Studies – Environmental Change, Linköping University, SE581 83 Linköping, Sweden

* Corresponding author: haji.mwevura@suza.ac.tz

†Author deceased

Abstract

Batch adsorption-desorption equilibrium techniques were used to investigate the adsorption capacity and influence of salinity on partitioning of the insecticide chlorpyrifos between water and soil or water and sediments from the Rufiji Delta. The data were fitted to different adsorption-desorption models and the hysteresis index was calculated using the ratio between the Freundlich exponents for desorption and adsorption, and secondly, the difference in area under the normalized adsorption and desorption isotherms using the maximum adsorbed and solution concentrations. The data showed non-linear adsorption and that chlorpyrifos was strongly adsorbed to soil and sediments from the Rufiji Delta. The linearized adsorption coefficient (K_D) and Freundlich adsorption coefficient (K_f) correlated significantly with organic carbon content. Chlorpyrifos adsorption as well as hysteresis calculated by both methods decreased with salinity (i.e. the sediment adsorbs increasing amounts of chlorpyrifos with decreasing salinity). This indicates that settling of freshwater sediments is among the major removal pathways of the chemical from the water column, but increased turbulence during high tides may resuspend settled sediment simultaneously increasing salinity and re-dissolve chlorpyrifos. However, discharge of fresh water, particularly during heavy rains, increases the trapping efficiency of the sediments. The theoretical approach developed showed that the Langmuir model describes the desorption data better than the Freundlich model, and that a better index of hysteresis is one that considers areas under the adsorption and desorption isotherms, provided the desorption isotherm is described by the normalized Langmuir isotherm and the adsorption isotherm by the normalized Freundlich isotherm.

Keywords: Hysteresis, Langmuir isotherm, Freundlich isotherm, Salinity, High tide,

Introduction

The Rufiji Delta supports the largest estuarine mangrove forest on the eastern seaboard of the African continent (UNEP, 2001). At 1,022 km^2, it hosts a rich biodiversity of both environmental and economic significance. The Rufiji Delta is considered a wetland of international importance under the 'Ramsar Convention on Wetlands' due to a unique biodiversity (Nasirwa *et al*., 2001). Economically, the delta is a very productive ecosystem supporting important fisheries and agricultural activities. The area accounts for 80% of all prawn catches in Tanzania (Mgana and Mahongo, 1997; Scheren *et al*., 2016) while agricultural activities are dominated by rice farming. Rice farming within the delta is described in the vernacular language as 'mangrove rice farming'.

Crabs foraging on the rice seedlings are considered a major problem by farmers engaged in mangrove rice farming. The use of pesticides and rice husks against the crabs is a common practice in rice fields within the mangrove forest of the Rufiji Delta (Standlinger *et al*., 2011). Many organophosphorous pesticides (OPPs) with high acute toxicity have been found in fairly high

http://dx.doi.org/10.4314/wiojms.v19i1.7

concentrations in water, soils and sediments from the delta water during the farming season (Mwevura, 2007), thus posing a threat to the aquatic ecosystem in the delta.

At low tide, the pesticides are spread, often together with rice husks as bait, in piles in the fields. The rising tide inundates the fields spreading the pesticides widely in the fields, but when the tide falls pesticides recede into the water of the delta. In spite of the obvious risks to the environment, the fate of pesticides in the Rufiji Delta, or similar environments in the tropics, has not been well investigated. A thorough understanding of the processes and the effects of environmental conditions is necessary for the prediction of pesticides movement and fate in the delta. Pesticide adsorption-desorption plays a major role in the environmental fate of pesticides. These processes have a major effect on the physical accessibility of the pollutants to microorganisms and affect a variety of other fate processes such as volatilization, bioavailability, photolysis, leaching and hydrolysis (Schwarzenbach *et al*., 2003).

The partitioning of an organic compound between water and particles is affected by a number of factors such as absorbent properties and the nature of the adsorbate, and the environmental variables. Adsorbent properties of soil or sediment that may considerably affect the adsorption of a given pesticide include organic matter and clay content, cation exchange capacity (CEC), pH, hydrous oxide content and metal ions (Schwarzenbach *et al*., 2003; Lu and Pignatello, 2004). Compound-specific physico-chemical properties of importance include water solubility, hydrophobicity, polarity, and acid-base properties (Schwarzenbach *et al*., 2003; Boethiling and Mackay, 2000). Properties of the aqueous phase, such as pH, and temperature (Hulscher and Cornelissen, 1996; Rani and Sud, 2015) are also important.

Apart from the factors that affect pesticide sorption in all environments, the salinity variations in a delta environment adds to the complexity. The salinity will vary both spatially, with lower salinity in the inner parts of the delta, and temporally, with tidal action. To understand the behavior of a pesticide within a delta it is therefore important to investigate the adsorption-desorption behavior and the partitioning of pesticides at different salinities.

Chlorpyrifos (O,O-diethyl-O-(3,5,6-trichloro-2-pyridinyl) phosphorothioate, CAS RN 2921-88-2) was found in high frequency and relatively high concentrations in the Rufiji Delta (Mwevura, 2007). It is an OPP with broad-spectrum insecticidal activity against a number of pests. Various formulations have been developed to maximize stability and contact with pests while minimizing human exposure. Four formulations, Dursban, Gladiator, Terraguard, and Pyrinex 48 EC02, have been registered in Tanzania, of which Dursban formulations are the most common. According to its registration status, chlorpyrifos is used against a wide range of insect pests including chewing and sucking insects and subterranean termites in coffee, rice and beans. It is also registered for control of sugarcane grubs as well as for use in public health programmes against mosquitoes (TPRI, 2020). Based on its low water solubility (1.4 mg/L) and high hydrophobicity (log K_{ow} = 5.27) chlorpyrifos partitions strongly to aquatic sediments and macrophytes where it can pose dangers to benthic organisms (Tomlin, 2006).

It is difficult to address the complexities of changing salinities found in the intertidal environment using the traditional methods of calculating adsorption coefficients and description of desorption isotherms. Development of the theoretical models to address the situation was therefore necessary. The present study elucidated the adsorption-desorption behavior of chlorpyrifos in soils and sediments and the influence of salinity variations on these processes. While evaluating the results, complexities were found that were not well described by traditional methods of calculating adsorption coefficients and description of desorption isotherms. The new approaches described in this paper should be useful in other contexts such as the estimation of sorbed pesticides in rice farms affected by coastal flooding.

Methodology

Sampling and sample handling

Soil and sediment samples were collected from two sites within rice farms (Ruaruke and Matosa) in the Rufiji Delta (Fig.1). Ruaruke is a relatively new cultivated area with rice farms established in 2002. The farms are located along the northern banks of the Kikunya River channel and are surrounded by dense mangrove stands. Farmers prefer to clear mangroves to create areas for new farms because of higher fertility and the absence of weeds. Matosa rice farms are among the oldest farms in the delta, established in the 1970s. They are located along the northern banks of the Simba Uranga River channel and are characterized by the presence of dense weeds.

Soil samples were collected on the farms while sediment samples were collected from riverbanks adjacent to the farms. Samples were collected by scooping the top layer (0-20 cm) using a stainless cylindrical spoon and then wrapped in aluminum foil. Soil and sediment samples were analyzed for physico-chemical parameters including pH, particle size, total carbon and organic carbon (OC) (Table 1; FAO, 2006).

The samples were air-dried at room temperature (<25°C), carefully ground in a mortar and sieved through a 2 mm sieve. The prepared samples were then stored in sealed glass containers until the adsorption-desorption experiments were conducted.

bration time. These experiments showed that a sorbent:solution ratio of 1:5 was ideal and equilibrium was established within 18 hrs of shaking. To make timing of the experiments easier, each batch of samples was shaken for 24 hrs.

Pesticide adsorption on soil from Ruaruke and Matosa, and sediments from Ruaruke were determined using the OECD standard batch equilibrium technique (OECD, 2000). The sorbent (2 g) was placed in a 25 ml Teflon tube with Teflon-lined screw cap and conditioned with the background solution (10 ml) by shaking overnight. The background solution was made up of $CaCl_2$ in deionized water (0.001 moles/l). ^{14}C-labe-

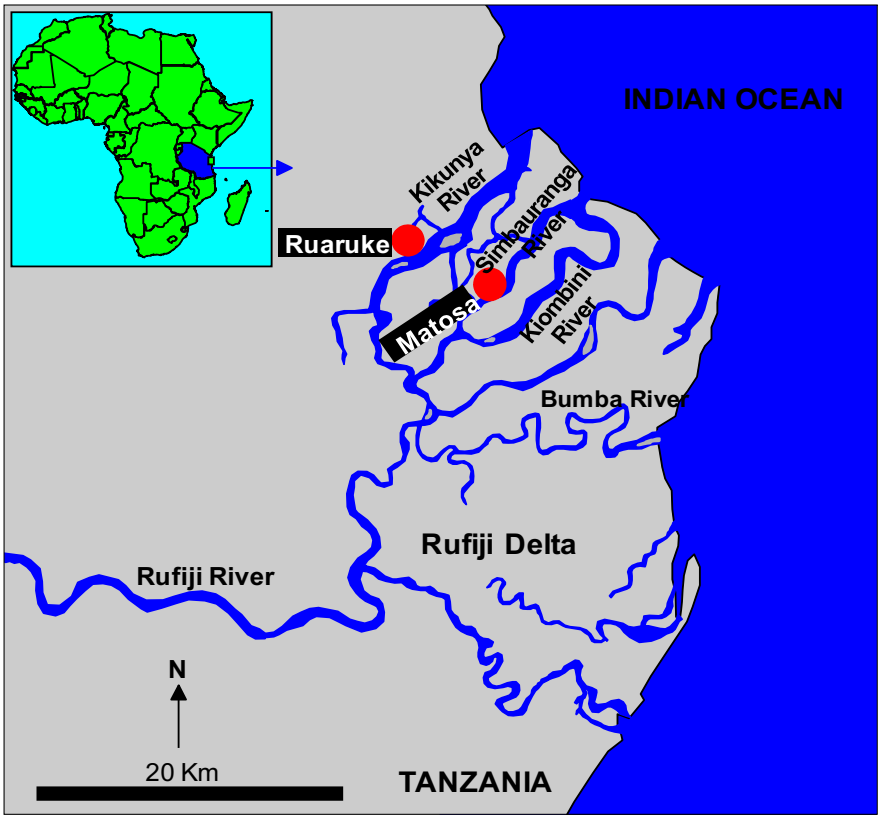

Figure 1. Map showing the location of study area and sampling sites (red dots).

Experimental procedure

Uniformly labeled ^{14}C-chlorpyrifos [pyridine-2,6-^{14}C] (purity 99%) from American Radiolabeled Chemicals, (St. Louise, MO, USA) was used. Calcium chloride ($CaCl_2$) and sodium chloride (NaCl) used were of analytical grade (Merck, Spånga, Sweden), while the water used was from a MilliQ purification system with an additional filtration through activated carbon.

Preliminary experiments were conducted to determine the optimum sorbent:solution ratio and equilibled chlorpyrifos was spiked to the conditioned mixture at four initial concentrations (0.056, 0.112, 0.168, 0.224 mg/l) in duplicate. These initial concentrations were achieved by spiking 12.5, 25, 37.5 and 50 ml of 112 mg/ml ^{14}C-labeled chlorpyrifos. The mixture was shaken for 24 hrs on a shaking table to equilibrate and then centrifuged at 3,500 rpm for 30 minutes. An aliquot (1 ml) of the supernatant was transferred to a scintillation vial with OptisafeHisafe 2 (Wallac, Turku, Finland) scintillation cocktail (5 ml). Radioactivity was quantified by liquid scintillation counting

(LKB Wallac 1217 Rackbeta). Internal standards from Wallac (C-14 Wallac product No. 1210-122) were used to correct for sample quenching. Blanks (no chlorpyrifos added) were run to correct for background radioactivity. The blank readings and conversion of radioactivity readings into concentrations of pesticide are presented in supplementary Table S1.

Adsorption – Desorption experiment using Ruaruke sediment

The air-dried sediments (2 g) were conditioned with 10 ml of low salinity background solution (0.001 moles/l$CaCl_2$ in deionised water) in the 25 ml Teflon centrifuge tubes by shaking overnight. Adsorption was initiated by spiking 10, 20, 30, 40 and 57 ml of 112 mg/ml ^{14}C-labeled chlorpyrifos into the conditioned sediment:solution mixture to give five initial concentrations of 0.045, 0.09, 0.135, 0.180 and 0.255 mg/l, respectively. Four replicates were used for each initial concentration. The mixtures were shaken for 24 hrs and centrifuged at 3,500 rpm for 30 minutes. An aliquot (1 ml) of the supernatant was processed for scintillation counter analysis as described in the adsorption experiment. The remaining supernatant was carefully decanted off immediately after removing the aliquot for the adsorption data.

The desorption experiments were conducted by successive dissolution techniques of the adsorbed material by adding fresh background solution (10 ml) free from pesticide. Each desorption cycle was conducted as described above. The adsorption-desorption procedure was repeated using background solutions of 0.001 moles/l $CaCl_2$ in water of 36 ‰ salinity to generate high salinity adsorption/desorption data.

Data analysis and interpretation

All adsorption data were fitted to the linear model (Eq. 1):

$$S = K_D C \qquad (1)$$

and to the log-transformed form of the Freundlich equation (Eq. 2):

$$\log S = \log K_f + N \log C \qquad (2)$$

Where S is the sorbed concentration (mg/kg), C is the aqueous phase concentration (mg/l), K_D (l/kg),K_f ($l^N mg^{1-N}$/kg) and N are constants (Schwarzenbach *et al.*, 2003). The Freundlich isotherms were plotted (log S against log C), and K_f and N were obtained from the slope and intercept of the isotherms. The desorption data were fitted to the Langmuir isotherm (Eq. 3):

$$S = \frac{S_{\max} kC}{1 + kC} \qquad (3)$$

Where S_{max}(mg/kg) is the maximum adsorption potential and k (l/mg) is the affinity coefficient.

Since K_D-values for the Freundlich isotherm are concentration dependent, several approaches were taken to linearize the isotherms and obtain K_D values that are not concentration dependent.

Assuming that the linear isotherm and the nonlinear isotherm have equal amounts of solute adsorbed at a given concentration *Cmax.*, K_{D1} is the linearized sorption coefficient (Eq. 5)

$$\int_0^{C\max} K_D C\, dc = \int_0^{C\max} K_f C^N dc \qquad (4)$$

$$K_{D1} = \frac{2K_f C\max^{N-1}}{N+1} \qquad (5)$$

Finding an average K_D from a nonlinear isotherm at C_{max}., K_{D2} is the linearized sorption coefficient (Eq. 6).

$$K_{D2} = \frac{\int_0^{C\max} K_f N C^{N-1}}{\int_0^{C\max} dC} dC = K_f C\max^{N-1} \qquad (6)$$

Using the $K_{D3} = NK_f$-value at C=1 (mg/l) from the relationship:

$$S = K_f C^N; K_{D3} = \frac{dS}{dC} = NK_f C\max^{N-1} \qquad (7)$$

Linearized sorption coefficients (K_{D1}, K_{D2} and K_{D3}) from the three approaches and K_D from the linear isotherm (Eq. 1) were then normalized to the organic carbon content of the corresponding sorbents to give K_{DOC}, K_{D1OC}, K_{D2OC} and K_{D3OC} that were used to compare between low and high saline soil and sediment samples.

The desorption data were fitted to the linear form of the Langmuir equation (Eq. 3) and the parameters S_{max} and k were calculated from the linear plot of C/S against C (Schwarzenbach, *et al.*, 2003). Similarly, the desorption data were also fitted to the Freundlich isotherm (Eq. 2).

Hysteresis indices (H) were calculated by two different methods. The first was to take the ratio between the Freundlich exponents for desorption and adsorption ($H = N_D/N_S$). If H = 1 there is no hysteresis, while a decreasing H (H < 1) indicates increased difficulty of the sorbed pesticide to desorb from the matrix, which is called positive hysteresis. Conversely,

Table 1. Physical and chemical properties of the tested soils and sediment.

	pH (1 mM Ca^{2+})	Sand %	Silt %	Clay %	Total C %	OC %
Ruaruke Soil (RSO)	7.0	24.3	23.6	52.1	2.05	1.96
Ruaruke Sediments (RSE)	7.2	28.5	25.2	46.3	1.32	1.24
Matosa Soil (MSO)	6.8	20.3	29.3	50.4	1.84	1.79

an increasing H (H > 1) is called negative hysteresis, which indicates that a sorbed substance is readily desorbed to solution (Huang and Weber, 1997; Chefetza *et al*., 2004). In the method described here, however, this is carried out for each desorption loop where there is no single index of hysteresis for a given set of experimental data.

In the second method, the adsorption and desorption data were normalized to the maximum adsorption point at equilibrium and fitted to the Langmuir or Freundlich equations for desorption and to the Freundlich equation for adsorption. The magnitude of the hysteresis was obtained by taking the area difference under the Langmuir or Freundlich fitted desorption curve and expressing it as a percentage of the area under the normalized adsorption Freundlich isotherm (Brown, 1994). The normalization technique coalesced the desorption loops into one and thus simplified the comparison of the two salinity conditions. This leads to $0 \leq H < 100$. When there is no hysteresis $H = 0$. The larger the value of H, the more hysteresis there is in the system.

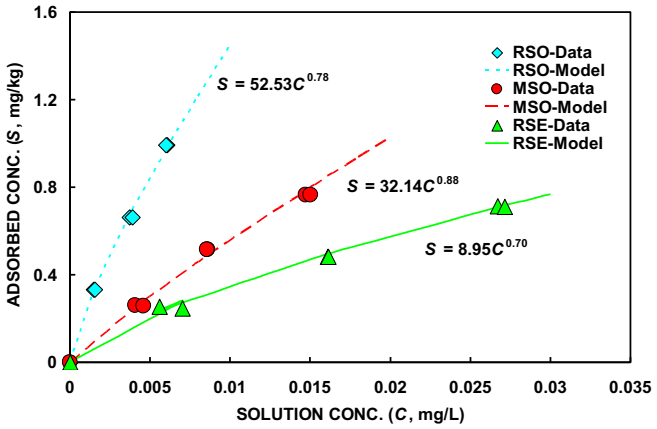

Figure 2. Chlorpyrifos adsorption isotherms for Ruaruke soil (RSO), Matosa soil (MSO), and Ruaruke sediment (RSE). 'Data' refers to the actual measurements, and 'model' to the isotherm calculated from the respective set of data.

Results and Discussion

Adsorption of chlorpyrifos

Soil and sediment properties from the two sites are given in Table 1. All samples were dominated by clay content which contributed between 46.3 and 52.1 % of the soil. The organic carbon and total carbon content ranged from 1.24 - 1.96 % and 1.32 to 2.05 %, respectively. The highest percentages of clay and organic carbon contents were measured in Ruaruke soil (RSO) followed by Matosa soil (MSO). Ruaruke sediment (RSE) gave the lowest percentages of clay and organic carbon content.

The results of chlorpyrifos adsorption experiments are summarized in Table 2. Nonlinear isotherms were obtained for all adsorbents indicating that chlorpyrifos has a preferential adsorption to soils and sediment initially, and adsorption decreases as more pesticide is adsorbed (Fig. 2). The adsorption data were better described with the Freundlich equation with R^2 values between 0.983 and 0.996 compared to R^2 values of the linear isotherms which were between 0.957 and 0.981. In a case like this the linear isotherm model should not be used to interpret the data since the slopes of the chlorpyrifos Freundlich isotherms (N) were less than 1. N values which indicate the dependence of adsorption on concentration were 0.78, 0.88 and 0.70 for RSO, MSO and RSE, respectively.

Effects of organic carbon and clay contents on adsorption

The linearized K_D values from the Freundlich isotherms indicated that RSO had higher adsorption capacity for chlorpyrifos than MSO while RSE had lower adsorption capacity than MSO. The linearized K_D values increased in the order RSE < MSO < RSO (Table 2). The adsorption parameters (normalized K_D and K_f) increased with increasing OC and clay contents (Table 1 and 2) indicating that the OC content was not the only factor responsible for the adsorption. Jeong *et al.* (2008) reported that the nature of the OC may influence adsorption. Dissolved OC particularly

affects the adsorption capacity of sediment in wetland areas and in turn the bioavailability of contaminants (Huang and Lee, 2001; Goedkoop and Peterson, 2003; Widenfalk, 2005). The trend of the linearized K_D values reflects the OC content of the respective sorbent (Tables 1 and 2). However, the carbon normalized adsorption coefficients (K_{DOC}, $K_{D1OC,}$ K_{D2OC}, and K_{D3OC}) had different values (Table 2). In particular K_{DOC} values were much larger than the other three. This is a result of using the wrong model of a linear isotherm. The other three approaches of linearized $K_D$were calculated at C = 1 µg/ml. In most investigations K_{OC} is calculated for nonlinear isotherms using K_f which is equivalent to using Eq. 6 at C_{max} = 1. The K_{OC} value is numerically equal to K_{OC} obtained with Eq. 6. Therefore Eq. 6 K_{OC} values are preferred. Interestingly, the trend in all calculated K_{OC} values was RSE < MSO < RSO. These observations suggest that a linear isotherm model should not be used to calculate K_{OC} if the isotherms are nonlinear, and that the acceptable linearized K_D model is one that calculates the average K_D at the equilibrium solution concentration (C) of interest. K_{OC} values determined in this study (722–2680) are within the lower range (1250–12600) reported in the literature (Tomlin, 2006).

As mentioned above, the adsorption coefficients also correlated with the clay contents (R^2 = 0.9963 for K_{D2}). In most investigations OC has been the more important factor for the adsorption of pesticides, while the clay content contributes significantly in soils with low OC content (Green and Karickhoff, 1990). The OC rich soil and sediment from the Rufiji Delta stand out to some extent in that the clay content contributes to the adsorption of chlorpyrifos. Thus, not only the quantity of the OC, but the quality and composition of the OC as well as the mineral component of the soil or sediment are of importance (Jeong *et al*., 2008; Kile *et al*., 1999; Mitra *et al*., 2003).

Table 2. Adsorption and desorption parameters of soil and sediment.

Adsorption							
	K_D L/kg	K_f $(L^N mg^{1-N})$/kg	N	K_{DOC} L/kg	K_{D1OC} L/kg	K_{D2OC} L/kg	K_{D3OC} L/kg
RSO[a]	169.74	52.53	0.78	8660	3011	2680	2090
MSO	53.95	32.14	0.88	3014	1910	1796	1580
RSE	27.86	8.59	0.70	2247	849	722	485
RSEL	37.86	26.93	0.91	3053	2274	2172	1976
RSEH	53.09	19.50	0.76	4281	1787	1573	1196

Desorption					
	Non-normalized: Freundlich			Non-normalized: Langmuir	
	K_{fd}	N_D	H	S_{max}	K
RSEL	0.37–1.31	0.11–0.09	0.12–0.08	0.21–0.99	3236–1125
RSEH	0.47–1.27	0.13–0.06	0.17–0.08	0.22–1.05	9099–1901
	Normalized: Freundlich			Normalized: Langmuir		
	K^*_{fd}	N^*_D	H	S^*_{max}	K^*	H
RSEL	1	0.08	0.09	1	27.03	73%
RSEH	1	0.06	0.08	1	39.10	59%

[a] RSO = Ruaruke soil; MSO = Matosa Soil; RSE = Ruaruke Sediment; RSEL = Ruaruke sediment, low salinity conditions; RSEH = Ruaruke sediment, high salinity conditions.

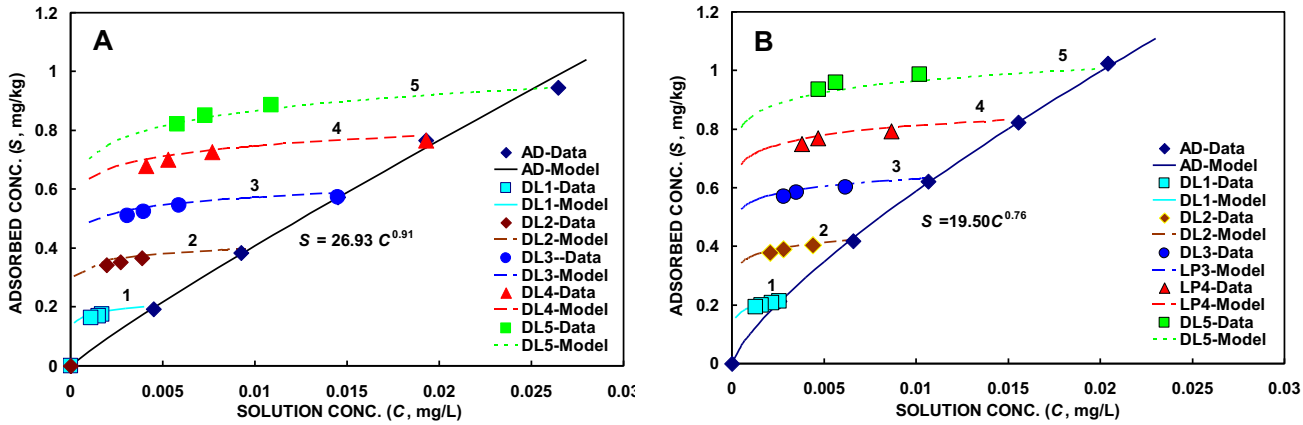

Figure 3. Non-normalized isotherms for chlorpyrifos adsorption-desorption in Ruaruke sediment. A=Low salinity, adsorption-Freundlich and desorption-Freundlich isotherms; B=High salinity, adsorption-Freundlich and desorption-Freundlich isotherms. AD refers to the adsorption phase and DL to the respective desorption loop. 'Data' refers to the actual measurements and 'model' to isotherms subsequently calculated from the data.

The strong adsorption of chlorpyrifos in both soils and sediment suggests that adsorption plays an important role in the overall fate of chlorpyrifos in the Rufiji Delta. Similarly, suspended sediment can absorb substantial amounts of chlorpyrifos in a wetland (Moore *et al.*, 2002) and more than 50% of the measured chlorpyrifos in aquatic bodies is associated with sediments.

Desorption and hysteresis

During adsorption the low salinity sediments (RSEL) adsorbed more chlorpyrifos than the high salinity sediments (RSEH) and both isotherms were nonlinear. The K_{OC} values calculated using Eq. 6 were 2172 and 1573 for RSEL and RSEH, respectively (Table 2). Under both low and high salinity conditions, the desorption data fit the Freundlich isotherm (Fig. 3). The desorption coefficient (K_{fd}) of the desorption loops increased as the initial equilibrium solution concentration increased, but the N_D values decreased (Fig. 3). Based on the Freundlich model for both adsorption and desorption isotherms, the hysteresis index average for all five loops was close to H = 0.1 for both RSEL and RSEH. Based on the method of calculating H that uses the N_D/N_S ratio, there was no difference in hysteresis between low salinity (H = 0.12 - 0.08) and high salinity (H = 0.17 - 0.08) sediment treatments.

The adsorption data were described by the Freundlich isotherm and the desorption data by the Langmuir isotherm (Fig. 4). Since desorption was initiated from the maximum equilibrium concentration of a given desorption loop, it is apparent that the Langmuir model is more appropriate than the Freundlich

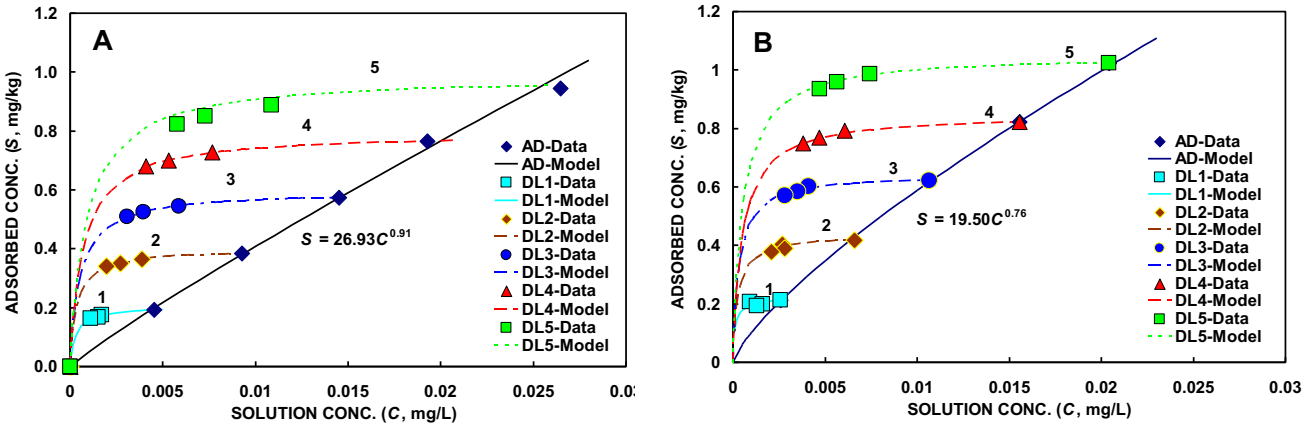

Figure 4. Non-normalized isotherms for chlorpyrifos adsorption-desorption in Ruaruke sediment. A=Low salinity, adsorption-Freundlich and desorption-Langmuir isotherms; B=High salinity, adsorption-Freundlich and desorption-Langmuir isotherms. AD refers to the adsorption phase and DL to the respective desorption loop. 'Data' refers to the actual measurements and 'model' to isotherms subsequently calculated from the data.

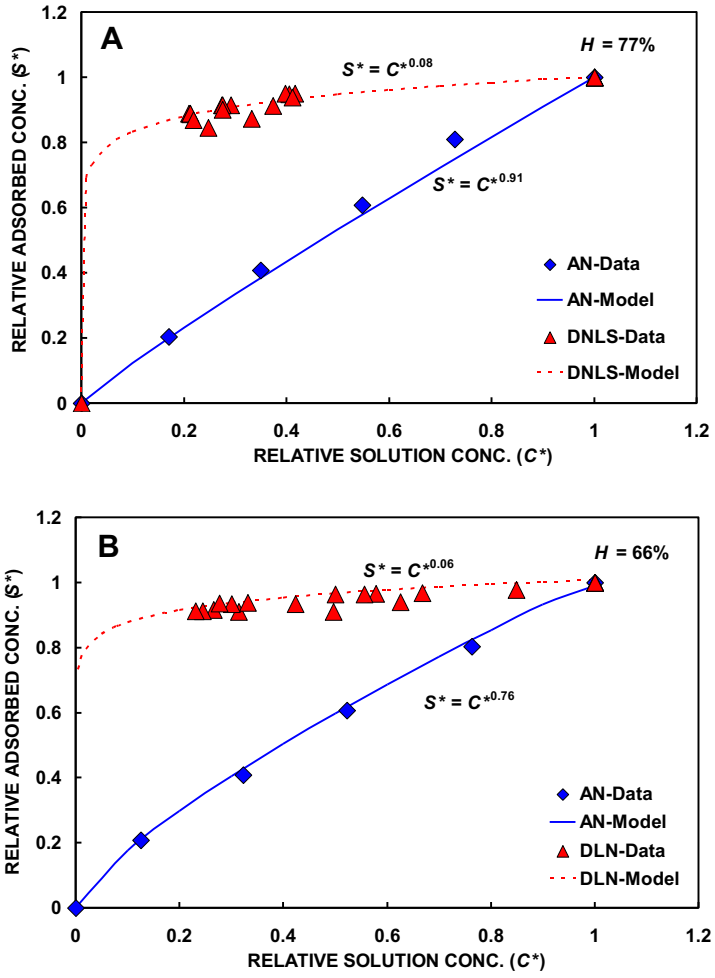

Figure 5. Normalized isotherms for Ruaruke sediment. A=Low salinity, adsorption-Freundlich and desorption-Freundlich isotherms; B=High salinity, adsorption-Freundlich and desorption-Freundlich isotherms.

model. It appears that the Langmuir model describes the desorption data better than the Freundlich model (Fig. 3 and 4). For both low and high salinity sediment treatments the S_{max} increases as the initial concentration of the desorption loops increases. However, the affinity coefficient (k) decreases with increase in initial concentration for desorption (Fig. 4 and Table 2).

The adsorption and desorption solution and adsorbed concentrations were normalized with the respective maximum concentration. The normalized data were then fitted to the Freundlich model (Fig. 5). For both low and high salinity sediment treatments, the desorption loops are described by one isotherm which has the desorption coefficient (K^*_{fd}) equal to 1 and N^*_D value that is close to the average of N_D values in Fig. 3. The normalized adsorption isotherm also has the adsorption coefficient (K^*_f) equal to 1 and the N^*_S value is the same as N_S for the non-normalized Freundlich isotherm (Fig. 3 and 5). Using data for the normalized Freundlich isotherms the hysteresis index $H = N^*_D / N^*_S$ is close 0.1. This implies that the normalization scheme averages the hysteresis indices for all five loops.

The hysteresis index was also calculated based on the areas under the normalized adsorption and desorption isotherms. The hysteresis index was 77 % for low salinity (RSEL) and 66 % for high salinity (RSEH). From the H values it is evident that the low salinity sediments had more hysteresis than the high salinity sediments. What is attractive about the normalization scheme and using the areas under the adsorption and desorption isotherms to calculate the hysteresis index is that both adsorption parameters (K_f and N_S) and desorption parameters (K_{fd}, and N_D) are incorporated into the normalized isotherms.

The normalization scheme was also carried out by using the Langmuir isotherm for desorption and the Freundlich isotherm for adsorption (Fig. 6). All five desorption isotherms coalesced into one desorption loop which had $S^*_{max} = 1$ for both RSEL and RSEH (Table 2). The calculated hysteresis index using areas under the adsorption and desorption normalized isotherms was 73 % for low salinity and 59 % for high salinity sediment treatments. It is believed that the difference in the calculated H indices using the normalized Freundlich and the Langmuir desorption isotherms is because the Freundlich model is not appropriate for desorption data. This can be seen in Fig. 5 in which the Freundlich isotherms abruptly go to $S^* = 0$ at normalized sorption concentration (S^*) of about 0.7. This abrupt approach to $C^* = 0$ over- estimates the area under the normalized desorption Freundlich isotherms which leads to an increase in the calculated H since the area under the normalized adsorption isotherm remains the same when the Freundlich or the Langmuir model is used. However, regardless of the model used to describe the normalized desorption isotherms the low salinity sediment had more hysteresis than the high salinity sediment. Based on these hysteresis data the normalized Langmuir isotherm is recommended for describing desorption isotherms and for calculating the hysteresis index.

Hysteresis is one of several manifestations of non-ideal adsorption behavior that challenge the assumptions associated with the application of adsorption models to the interaction of hydrophobic organic chemicals with adsorbent (Huang *et al.*, 1998). The adsorption-desorption behavior of chlorpyrifos at

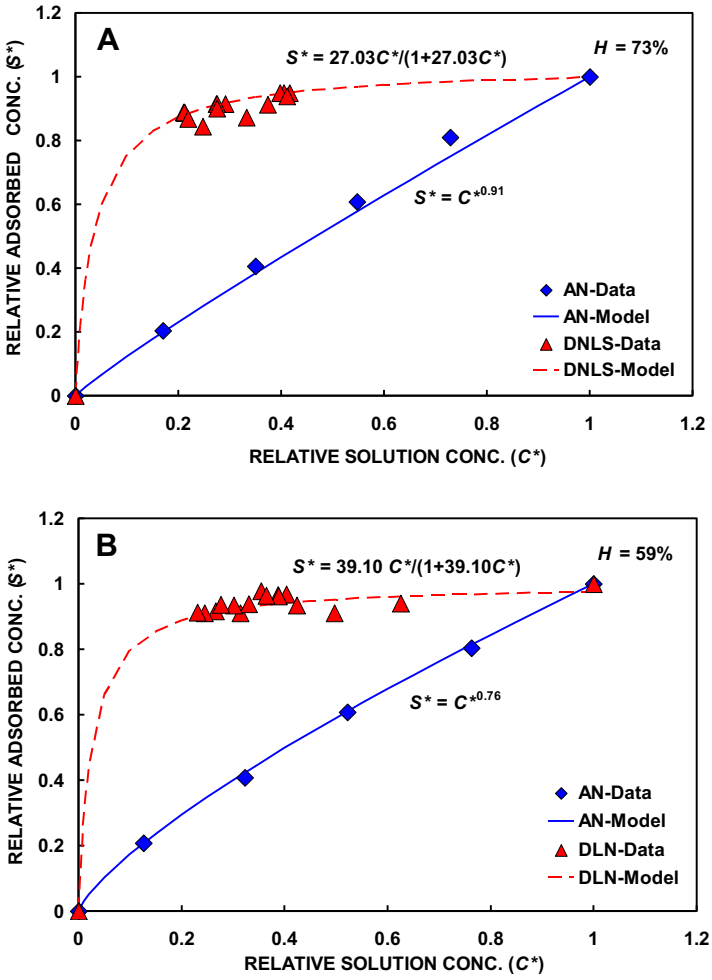

Figure 6. Normalized isotherms for Ruaruke sediment. A=Low salinity, adsorption-Freundlich and desorption-Langmuir isotherms; B=High salinity, adsorption-Freundlich and desorption-Langmuir isotherms.

both high and low salinity exhibited hysteresis indicating that the adsorption interactions are not truly reversible (Fig. 3 and 4). The amount of chlorpyrifos desorbed from the sediments was less than the amount adsorbed. This phenomenon may be caused by several factors including changes in solution composition and irreversible binding of chlorpyrifos to the sediments. Not attaining equilibrium during the desorption process could also contribute to hysteresis as the rate of desorption is slow (Mersie and Seybold, 1996; Amankwah, 2003; Kleineidam *et al*., 2004) and it has been shown that both hysteresis and non-linear adsorption are enhanced by cross-linking with aluminum ions (Al^{3+}) in the sorbent material (Lu and Pignatello, 2004). The difference between the adsorption and desorption processes is expressed in the hysteresis index values (H) summarized in Table 2. On average, the H decreased with increasing salinity, indicating that sediments in fresh water are better at sequestering chlorpyrifos than sediments in a saline water environment.

It is clear that the methods used to calculate sorption coefficients are very critical when discussing adsorption and desorption data. If the isotherm is nonlinear, using the sorption coefficient from the linear isotherm model can yield erroneous conclusions. For example, in Table 2, the K_D value for the high salinity sediment is larger than that for the low salinity sediment. However, using the linearized K_{D2}, the low salinity sediment adsorbed chlorpyrifos more strongly than the high salinity sediment. This leads to the over-estimation of K_{OC} when the linear isotherm model is used (Table 2). Similarly, using the Freundlich isotherm model for desorption showed that there was no difference in hysteresis between RSEL and RSEH if the hysteresis index is calculated based on N values for adsorption and desorption. Therefore, the index $H = N_D/N_S$ might not be appropriate because this method does not include the adsorption and desorption coefficients. A better index of hysteresis is one that considers areas under the normalized adsorption and desorption isotherms, provided the desorption isotherm is described by the normalized Langmuir isotherm. This method of calculating H incorporates all adsorption (K_f and N) and desorption (S_{max}, and k) parameters. Based on the normalized Langmuir desorption isotherm and the Freundlich normalized adsorption isotherm, the low salinity sediments exhibited more hysteresis than the high salinity sediment (Table 2).

Concluding remarks

The results from this study show that chlorpyrifos was strongly adsorbed in sediments and soils from the Rufiji Delta and therefore adsorption and settling of sediments are among the major removal pathways of the chemical from the water column. The adsorption process was found to be nonlinear, and, contrary to what was expected, the organic carbon content was not the only adsorbent parameter that influenced chlorpyrifos adsorption, suggesting that other adsorbent components such as clay content were also responsible for adsorption of chlorpyrifos. When calculating K_{OC} values a correct model for describing adsorption isotherms must be used. If the isotherm is nonlinear then the linear isotherm model should not be used. However, for a nonlinear isotherm a justifiable linearization method is one that calculates the average K_D within the range of solution concentration (0 to C). The value of C has been taken to be $C = 1$ µg/ml by many researchers. This leads to using K_f in Eq. 7 to calculate

K_{OC}. Adsorption-desorption hysteresis was observed in sediments under both low and high salinity conditions. The extent of chlorpyrifos adsorption on the sorbents tested, as well as hysteresis calculated in different methods, decreased with salinity, implying that under freshwater conditions, sediments play a more important role in trapping chlorpyrifos than in saline water sediments. The finding that chlorpyrifos adsorbs more at low than high salinity is puzzling. A salting out effect that lowers the solubility of the compound with higher salt concentration would have been plausible (Means, 1995). The explanation may lie in competition for adsorptive sites between chlorpyrifos and ions at higher cation exchange capacity (CEC). Additional studies are needed to confirm these findings.

Acknowledgments

Anna Hellström and Lutufyo Mwamtobe gave technical assistance. This work was carried out with grants from the International Programmes in Chemical Sciences (IPICS), Uppsala University, Sweden, and the Western Indian Ocean Marine Science Association (WIOMSA). Soil analyses and scintillation counting were performed at the Department of Soil Sciences, Swedish University of Agricultural Sciences.

References

Amankwah EA (2003) Modelling of sorption and desorption hysteresis phenomena. PhD Thesis, Eberhard - Karls – Universität Tübingen, Germany. 203 pp

Boethiling RS, Mackay D (2000) Handbook of property estimation methods for chemicals – Environmental and Health Sciences. Lewis Publishers, London, UK. 492 pp

Brown KD (1994) Sorption and Degradation of Atrazine, Diuron, and Carbaryl in single and multi-pesticides Systems. MSc Thesis, University of Florida, USA. 127 pp

Chefetza B, Bilkisb YI, Polubesova T (2004) Sorption–desorption behavior of triazine and phenylurea herbicides in Kishon River sediments. Water Research 38: 4383-4394 [doi:10.1016/j.watres.2004.08.023]

FAO (2006) Guidelines for soil description, 4th ed. Food and Agricultural Organisation, Rome, Italy. 97 pp

Goedkoop W, Peterson M (2003) The fate, distribution, and toxicity of lindane in tests with *Chironomusriparius* – effects of bioturbation and sediment organic matter content. *Environmental Toxicology and Chemistry* 22: 67–76 [doi:10.1897/1551-5028(2003)022<0067:TFDATO>2.0.CO;2]

Green RE, Karickhoff SW (1990) Sorption estimate for modeling. In: Cheng HH, Madison WI (eds) Pesticides in the soil environment. Soil Science Society of America. pp 79-101

Huang W, Weber WW (1997) A distributed reactivity model for sorption by soil and sediments: Relationships between desorption hysteresis and the chemical characteristics of organic domains. Environmental Science Technology 31: 2562–2585 [doi:10.1021/es960995e]

Huang W, Yu H, Weber WW (1998) Hysteresis in the sorption and desorption of hydrophobic organic contaminants by soils and sediments: A comparative analysis of experimental protocol. Journal of Contaminant Hydrology 31: 129–148 [doi:10.1016/S0169-7722(97)00056-9]

Huang X, Lee LS (2001) Effects of dissolved organic matter from animal waste effluent on chlorpyrifos sorption by soils. Journal of Environmental Quality 30: 1258-1265

Hulscher TEM, Cornelissen G (1996) Effect of temperature on sorption equilibrium and sorption kinetics of organic micro-pollutants – A review. Chemosphere 32: 609–626 [doi:10.1016/0045-6535(95)00345-2]

Jeong S, Wander M, Kleineidam S, Grathwohl P, Ligouis B, Werth CJ (2008) The role of condensed carbonaceous materials on the sorption of hydrophobic organic contaminants in subsurface sediments. Environmental Science and Technology 42:1458-1464 [doi: 10.1021/es0719879]

Kile DE, Wershaw RL, Chiou CT (1999) Correlation of soil and sediment organic matter polarity to aqueous sorption of organic compounds. Environmental Science and Technology 33: 2053-2056 [**doi:** 10.1021/es980816o]

Kleineidam S, Rugner H, Rathwohl P (2004) Desorption kinetics of phenanthrene in aquifer material lacks hysteresis. Environmental Science and Technology 38: 4169-4175 [doi**:** 10.1021/es034846p]

Lu Y, Pignatello JJ (2004) Sorption of polar aromatic compounds to soil humic acid particles affected by aluminum (III) ion cross-linking. Journal Environmental Quality 33: 1314-1321

Means JC (1995) Influence of salinity upon sediment-water partitioning of aromatic hydrocarbons. Marine Chemistry 51: 3-16 [doi:10.1016/0304-4203(95)00043-Q]

Mersie W, Seybold C (1996) Adsorption and desorption of atrazine, deethylatrazine, deisopropylatrazine and hydroxyatrazine on levy wetland soil. Journal of Agriculture and Food Chemistry 44: 1925-1929 [doi:10.1021/jf950370k]

Mgana S, Mahongo SB (1997) Land based sources affecting the quality and uses of the marine, coastal and

associated freshwater environment: Tanzania Mainland. Proceedings of UNEP Regional Workshop, Institute of Marine Sciences, Zanzibar. 50 pp

Mitra S, Bhowmik PC, Xing B (2003) Effects of soil physical and chemical properties on the sorption-desorption hysteresis of the diketonitrile metabolite of isoxaflutole. Weed Biology Management 3: 128-136 [doi: 10.1046/j.1445-6664.2003.00094.x]

Moore MT, Schulz R, Cooper CM, Smith S, Rodgers JH (2002) Mitigation of chlorpyrifos runoff using constructed wetlands. Chemosphere 46: 827-835 [doi:10.1016/S0045-6535(01)00189-8]

Mwevura H (2007) Chemodynamics of pesticide residues and other persistent organic pollutants within the Rufiji Delta and dolphins from the coastal waters of Zanzibar. PhD Thesis, University of Dar es Salaam, Tanzania. 330 pp

Nasirwa O, Owino A, Munguya E, Washira, J (2001) Waterbird counts in the Rufiji Delta. Rufiji Environment Management Project, Technical Report No. 24. 18 pp

OECD (2000) Adsorption-desorption using a batch equilibrium method. Organization for Economic Cooperation and Development, guideline for the testing of Chemicals 106. 45 pp

Rani S, Sud D (2015) Effect of temperature on adsorption-desorption behaviour of triazophos in Indian soils. Plant and Soil Environment 61: 36-42

Scheren P, Diop S, Machiwa J, Ducrotoy JP (2016) The Western Indian Ocean: a wealth of life-supporting ecosystem goods and services. Estuaries: A lifeline of ecosystem services in the Western Indian Ocean. Springer. pp 1-23

Schwarzenbach RP, Gschwend PM, Imboden DM (2003) Environmental organic chemistry, 2nd ed. Wiley-Interscience, John Wiley & Sons, Inc., NY. 1328 pp

Stadlinger N, Mmochi AJ, Dobo S, Gyllbäck E, Kumblad L (2011) Pesticide use among smallholder rice farmers in Tanzania. Environment, Development and Sustainability 13: 641-656

TPRI (2020) Registered pesticides for use in the United Republic of Tanzania. Tropical Pesticides Research Institute, Arusha, Tanzania

Tomlin, CDS (ed) (2006) A world compendium: The pesticide manual, 14th ed. British Crop Protection Council, Surrey, UK. 1250 pp

UNEP (2001) Eastern African atlas of coastal resources: Tanzania. United Nations Environmental Programme, Nairobi, Kenya. 111 pp

Widenfalk A (2005) Interactions between Pesticides and microorganisms in freshwater sediments: Toxic effects and implications for bioavailability. PhD Thesis, Swedish University of Agricultural Sciences, Uppsala, Sweden. 38 pp

Calculations

Concentration of Chlorpyrifos in analysed supernantant (Cw, µg/ml) was calculated using the following formula:

$$Cw = \frac{\text{Net radioactivity reading of supernatant X Conc. of original solution}}{\text{radioactivity reading of original solution}}$$

$$Cw = \frac{\text{(A B) X Co}}{\text{Ro}}$$

Original Mass of chlorpyrifos (Mo) = Co x volume of Solution (V)

Mo = Co x V

Mass of chlorpyrifos in the supernatant (Mw) = Cw x volume of Solution (V)

Mw = Cw x V

Mass of chlorpyrifos in the adsorbed in soil/sediment (Ms) = Mo - Mw

$$\text{Concentration of chlorpyrifos (Cs , µg/g = mg/kg)} = \frac{\text{Mass of chlorpyrifos in soil/sediment (Ms)}}{\textit{Mass of soil/sediment}}$$

$$\text{Cs (µg/g = mg/kg)} = \frac{\text{Ms}}{ms}$$

Data from adsorption experiment using Ruaruke Soil (RSO) , Matosa Soil (MSO) and Ruaruke Sediments (RSE)

Sorbate (ms = 2g)	Sample	Radioactivity Readings disintegration per minute (dpm)				Volume	Original Conc	Original Mass	Conc. supernatant	Mass in supernatant	Mass adsorbed	Conc adsorbed
		Sample (A)	Blank (B)	Net (A-B)	Original Solution (Ro)	V(mls)	Co (µg/ml)	(Mo) VCo(µg)	Cw	Mw CwV	Ms (Mo - Mw)	Cs (Ms/ms)
RSO	C1A	860.53	51.15	809.38	11106.36	10	0.055942	0.55942	0.004077	0.040768	0.518652	0.259326
	C1B	961.03	51.15	909.88	11106.36	10	0.055942	0.55942	0.004583	0.04583	0.513589	0.256795
	C2A	1755.57	51.15	1704.42	22212.71	10	0.111884	1.118839	0.008585	0.08585	1.032989	0.516494
	C2B	1753.51	51.15	1702.36	22212.71	10	0.111884	1.118839	0.008575	0.085747	1.033092	0.516546
	C3A	2975	51.15	2923.85	33319.07	10	0.167826	1.678259	0.014727	0.147272	1.530986	0.765493
	C3B	3033.82	51.15	2982.67	33319.07	10	0.167826	1.678259	0.015024	0.150235	1.528024	0.764012
MSO	C1A	369.82	79.35	290.47	13556.24	10	0.068282	0.682818	0.001463	0.014631	0.668188	0.334094
	C1B	388.64	79.35	309.29	13556.24	10	0.068282	0.682818	0.001558	0.015579	0.66724	0.33362
	C2A	818.53	79.35	739.18	27112.47	10	0.136564	1.365637	0.003723	0.037232	1.328405	0.664202
	C2B	855.5	79.35	776.15	27112.47	10	0.136564	1.365637	0.003909	0.039094	1.326542	0.663271
	C3A	1280.94	79.35	1201.59	40668.71	10	0.204845	2.048455	0.006052	0.060523	1.987932	0.993966
	C3B	1271.36	79.35	1192.01	40668.71	10	0.204845	2.048455	0.006004	0.060041	1.988414	0.994207
RSE	C1A	1473.29	80.06	1393.23	11203.22	10	0.05643	0.564298	0.007018	0.070176	0.494122	0.247061
	C1B	1191.19	80.06	1111.13	11203.22	10	0.05643	0.564298	0.005597	0.055967	0.508331	0.254166
	C2A	3270.86	80.06	3190.8	22406.43	10	0.11286	1.128597	0.016072	0.160718	0.967878	0.483939
	C2B	3280.08	80.06	3200.02	22406.43	10	0.11286	1.128597	0.016118	0.161183	0.967414	0.483707
	C3A	5379.82	80.06	5299.76	33609.65	10	0.169289	1.692895	0.026695	0.266945	1.42595	0.712975
	C3B	5467.65	80.06	5387.59	33609.65	10	0.169289	1.692895	0.027137	0.271369	1.421526	0.710763

Sorption-desorption experiment

A: Data from adsorption-desorption experiment using Ruaruke Sediments (RSE, ms = 2g) at low salinity conditions.

Sorption Day zero	Radioactivity Readings disintegration per minute (dpm)				Volume	Original Conc	Original Mass	Conc. supernatant	Mass in supernatant	Mass adsorbed	Conc adsorbed
Sample	Supernatant (A)	V(mls)	Co (µg/ml)	(Mo) VCo(µg)	Cw	Mw CwV	Ms (Mo - Mw)	Cs (Ms/ms)	Mw CwV	Ms (Mo - Mw)	Cs (Ms/ms)
1CA1	1480.42	97.2	1383.22	8558.83	10	0.04311	0.431102	0.006967	0.069672	0.361431	0.180715
1CA2	**983.59**	97.2	886.39	8558.83	10	0.04311	0.431102	0.004465	0.044647	0.386456	0.193228
1CB1	1000.44	97.2	903.24	8558.83	10	0.04311	0.431102	0.00455	0.045496	0.385607	0.192803
1CB2	**1527.99**	97.2	1430.79	8558.83	10	0.04311	0.431102	0.007207	0.072068	0.359035	0.179517
2CA1	1900.54	97.2	1803.34	17117.66	10	0.08622	0.862205	0.009083	0.090833	0.771372	0.385686
2CA2	1946.43	97.2	1849.23	17117.66	10	0.08622	0.862205	0.009314	0.093144	0.76906	0.38453
2CB1	1908.76	97.2	1811.56	17117.66	10	0.08622	0.862205	0.009125	0.091247	0.770958	0.385479
2CB2	1984.43	97.2	1887.23	17117.66	10	0.08622	0.862205	0.009506	0.095058	0.767146	0.383573
3CA1	3005.15	97.2	2907.95	25676.49	10	0.129331	1.293307	0.014647	0.146471	1.146836	0.573418
3CA2	3026.08	97.2	2928.88	25676.49	10	0.129331	1.293307	0.014753	0.147526	1.145782	0.572891
3CB1	2973.68	97.2	2876.48	25676.49	10	0.129331	1.293307	0.014489	0.144886	1.148421	0.57421
3CB2	2894.71	97.2	2797.51	25676.49	10	0.129331	1.293307	0.014091	0.140909	1.152399	0.576199
4CA1	4021.70	97.2	3924.5	34235.32	10	0.172441	1.72441	0.019767	0.197674	1.526735	0.763368
4CA2	4065.00	97.2	3967.8	34235.32	10	0.172441	1.72441	0.019986	0.199855	1.524554	0.762277
4CB1	3832.20	97.2	3735	34235.32	10	0.172441	1.72441	0.018813	0.188129	1.53628	0.76814
4CB2	3776.57	97.2	3679.37	34235.32	10	0.172441	1.72441	0.018533	0.185327	1.539082	0.769541
5CA1	5384.15	97.2	5286.95	42794.15	10	0.215551	2.155512	0.02663	0.2663	1.889212	0.944606
5CA2	5315.37	97.2	5218.17	42794.15	10	0.215551	2.155512	0.026284	0.262836	1.892676	0.946338
5CB1	5637.80	97.2	5540.6	42794.15	10	0.215551	2.155512	0.027908	0.279076	1.876436	0.938218
5CB2	5650.21	97.2	5553.01	42794.15	10	0.215551	2.155512	0.02797	0.279701	1.875811	0.937905

Desorption Day 1	Radioactivity Readings disintegration per minute (dpm)				Volume	Original Conc	Original Mass	Conc. supernatant	Mass in supernatant	Mass adsorbed	Conc adsorbed
Sample	Supernatant (A)	V(mls)	Co (µg/ml)	(Mo) VCo(µg)	Cw	Mw CwV	Ms (Mo - Mw)	Cs (Ms/ms)	Mw CwV	Ms (Mo - Mw)	Cs (Ms/ms)
1CA1	497.56	160.77	336.79	15559.73	10	0.078373	0.361431	0.001696	0.016964	0.344467	0.172233
1CA2	496.53	160.77	335.76	15559.73	10	0.078373	0.386456	0.001691	0.016912	0.369544	0.184772
1CB1	502.80	160.77	342.03	15559.73	10	0.078373	0.385607	0.001723	0.017228	0.368379	0.18419
1CB2	808.56	160.77	647.79	15559.73	10	0.078373	0.359035	0.003263	0.032629	0.326406	0.163203
2CA1	888.18	160.77	727.41	15559.73	10	0.078373	0.771372	0.003664	0.036639	0.734733	0.367366
2CA2	927.25	160.77	766.48	15559.73	10	0.078373	0.76906	0.003861	0.038607	0.730453	0.365227
2CB1	947.14	160.77	786.37	15559.73	10	0.078373	0.770958	0.003961	0.039609	0.731349	0.365674
2CB2	943.87	160.77	783.1	15559.73	10	0.078373	0.767146	0.003944	0.039444	0.727702	0.363851
3CA1	1353.75	160.77	1192.98	15559.73	10	0.078373	1.146836	0.006009	0.06009	1.086746	0.543373
3CA2	1378.09	160.77	1217.32	15559.73	10	0.078373	1.145782	0.006132	0.061316	1.084466	0.542233
3CB1	1277.03	160.77	1116.26	15559.73	10	0.078373	1.148421	0.005623	0.056225	1.092196	0.546098
3CB2	1294.72	160.77	1133.95	15559.73	10	0.078373	1.152399	0.005712	0.057116	1.095282	0.547641
4CA1	1688.97	160.77	1528.2	15559.73	10	0.078373	1.526735	0.007697	0.076974	1.449761	0.72488
4CA2	1742.75	160.77	1581.98	15559.73	10	0.078373	1.524554	0.007968	0.079683	1.444871	0.722436
4CB1	1637.56	160.77	1476.79	15559.73	10	0.078373	1.53628	0.007438	0.074385	1.461895	0.730948
4CB2	1666.83	160.77	1506.06	15559.73	10	0.078373	1.539082	0.007586	0.075859	1.463223	0.731612
5CA1	2228.79	160.77	2068.02	15559.73	10	0.078373	1.889212	0.010416	0.104165	1.785047	0.892524
5CA2	2245.24	160.77	2084.47	15559.73	10	0.078373	1.892676	0.010499	0.104993	1.787683	0.893842
5CB1	2414.97	160.77	2254.2	15559.73	10	0.078373	1.876436	0.011354	0.113543	1.762893	0.881447
5CB2	2387.61	160.77	2226.84	15559.73	10	0.078373	1.875811	0.011216	0.112164	1.763646	0.881823

Desorption Day 2	Radioactivity Readings disintegration per minute (dpm)				Volume	Original Conc	Original Mass	Conc. supernatant	Mass in supernatant	Mass adsorbed	Conc adsorbed
Sample	Supernatant (A)	V(mls)	Co (µg/ml)	(Mo) VCo(µg)	Cw	Mw CwV	Ms (Mo - Mw)	Cs (Ms/ms)	Mw CwV	Ms (Mo - Mw)	Cs (Ms/ms)
1CA1	379.82	70.29	309.53	15042.31	10	0.075767	0.344467	0.001559	0.015591	0.328876	0.164438
1CA2	367.87	70.29	297.58	15042.31	10	0.075767	0.369544	0.001499	0.014989	0.354555	0.177277
1CB1	356.49	70.29	286.2	15042.31	10	0.075767	0.368379	0.001442	0.014416	0.353963	0.176982
1CB2	366.01	70.29	295.72	15042.31	10	0.075767	0.326406	0.00149	0.014895	0.311511	0.155755
2CA1	582.36	70.29	512.07	15042.31	10	0.075767	0.734733	0.002579	0.025793	0.70894	0.35447
2CA2	573.93	70.29	503.64	15042.31	10	0.075767	0.730453	0.002537	0.025368	0.705085	0.352543
2CB1	632.80	70.29	562.51	15042.31	10	0.075767	0.731349	0.002833	0.028333	0.703016	0.351508
2CB2	632.80	70.29	562.51	15042.31	10	0.075767	0.727702	0.002833	0.028333	0.699369	0.349684
3CA1	862.85	70.29	792.56	15042.31	10	0.075767	1.086746	0.003992	0.039921	1.046826	0.523413
3CA2	872.80	70.29	802.51	15042.31	10	0.075767	1.084466	0.004042	0.040422	1.044044	0.522022
3CB1	852.49	70.29	782.2	15042.31	10	0.075767	1.092196	0.00394	0.039399	1.052797	0.526398
3CB2	841.99	70.29	771.7	15042.31	10	0.075767	1.095282	0.003887	0.03887	1.056412	0.528206
4CA1	1141.35	70.29	1071.06	15042.31	10	0.075767	1.449761	0.005395	0.053949	1.395812	0.697906
4CA2	1118.08	70.29	1047.79	15042.31	10	0.075767	1.444871	0.005278	0.052776	1.392095	0.696047
4CB1	1110.87	70.29	1040.58	15042.31	10	0.075767	1.461895	0.005241	0.052413	1.409482	0.704741
4CB2	1118.56	70.29	1048.27	15042.31	10	0.075767	1.463223	0.00528	0.052801	1.410423	0.705211
5CA1	1470.30	70.29	1400.01	15042.31	10	0.075767	1.785047	0.007052	0.070518	1.71453	0.857265
5CA2	1467.28	70.29	1396.99	15042.31	10	0.075767	1.787683	0.007037	0.070365	1.717318	0.858659
5CB1	1560.41	70.29	1490.12	15042.31	10	0.075767	1.762893	0.007506	0.075056	1.687837	0.843919
5CB2	1569.45	70.29	1499.16	15042.31	10	0.075767	1.763646	0.007551	0.075512	1.688135	0.844067

Desorption Day 3	**Radioactivity Readings disintegration per minute (dpm)**				**Volume**	**Original Conc**	**Original Mass**	**Conc. supernatant**	**Mass in supernatant**	**Mass adsorbed**	**Conc adsorbed**
Sample	**Supernatant** (A)	V(mls)	Co (µg/ml)	(Mo) VCo(µg)	Cw	Mw CwV	Ms (Mo - Mw)	Cs (Ms/ms)	Mw CwV	Ms (Mo - Mw)	Cs (Ms/ms)
1CA1	299.12	103.53	195.59	14579.71	10	0.073437	0.328876	0.000985	0.009852	0.319024	0.159512
1CA2	327.97	103.53	224.44	14579.71	10	0.073437	0.354555	0.00113	0.011305	0.34325	0.171625
1CB1	370.2	103.53	266.67	14579.71	10	0.073437	0.353963	0.001343	0.013432	0.340531	0.170266
1CB2	300.81	103.53	197.28	14579.71	10	0.073437	0.311511	0.000994	0.009937	0.301574	0.150787
2CA1	455.53	103.53	352	14579.71	10	0.073437	0.70894	0.001773	0.01773	0.69121	0.345605
2CA2	448.19	103.53	344.66	14579.71	10	0.073437	0.705085	0.001736	0.01736	0.687725	0.343863
2CB1	518.76	103.53	415.23	14579.71	10	0.073437	0.703016	0.002091	0.020915	0.682101	0.34105
2CB2	533.06	103.53	429.53	14579.71	10	0.073437	0.699369	0.002164	0.021635	0.677734	0.338867
3CA1	727.64	103.53	624.11	14579.71	10	0.073437	1.046826	0.003144	0.031436	1.01539	0.507695
3CA2	737.53	103.53	634	14579.71	10	0.073437	1.044044	0.003193	0.031934	1.01211	0.506055
3CB1	693.39	103.53	589.86	14579.71	10	0.073437	1.052797	0.002971	0.029711	1.023086	0.511543
3CB2	702.97	103.53	599.44	14579.71	10	0.073437	1.056412	0.003019	0.030193	1.026219	0.513109
4CA1	928.71	103.53	825.18	14579.71	10	0.073437	1.395812	0.004156	0.041564	1.354249	0.677124
4CA2	908.46	103.53	804.93	14579.71	10	0.073437	1.392095	0.004054	0.040544	1.351551	0.675775
4CB1	908.35	103.53	804.82	14579.71	10	0.073437	1.409482	0.004054	0.040538	1.368944	0.684472
4CB2	911.2	103.53	807.67	14579.71	10	0.073437	1.410423	0.004068	0.040682	1.369741	0.68487
5CA1	1208.36	103.53	1104.83	14579.71	10	0.073437	1.71453	0.005565	0.05565	1.65888	0.82944
5CA2	1207.92	103.53	1104.39	14579.71	10	0.073437	1.717318	0.005563	0.055627	1.66169	0.830845
5CB1	1293.03	103.53	1189.5	14579.71	10	0.073437	1.687837	0.005991	0.059914	1.627923	0.813961
5CB2	1291.66	103.53	1188.13	14579.71	10	0.073437	1.688135	0.005985	0.059845	1.628289	0.814145

B: Data from adsorption-desorption experiment using Ruaruke Sediments (RSE, ms = 2g) at high salinity conditions.

Day zero Sorption	Radioactivity Readings disintegration per minute (dpm)				Volume	Original Conc	Original Mass	Conc. supernatant	Mass in supernatant	Mass adsorbed	Conc adsorbed
Sample	Supernatant (A)	V(mls)	Co (µg/ml)	(Mo) VCo(µg)	Cw	Mw CwV	Ms (Mo - Mw)	Cs (Ms/ms)	Mw CwV	Ms (Mo - Mw)	Cs (Ms/ms)
1CA1	591.87	102.4	489.47	8943.075	10	0.045046	0.450457	0.002465	0.024654	0.425802	0.212901
1CA2	594.09	102.4	491.69	8943.075	10	0.045046	0.450457	0.002477	0.024766	0.425691	0.212845
1CB1	664.51	102.4	562.11	8943.075	10	0.045046	0.450457	0.002831	0.028313	0.422143	0.211072
1CB2	593.26	102.4	490.86	8943.075	10	0.045046	0.450457	0.002472	0.024724	0.425732	0.212866
2CA1	1420.45	102.4	1318.05	17886.15	10	0.090091	0.900913	0.006639	0.066389	0.834524	0.417262
2CA2	1412.84	102.4	1310.44	17886.15	10	0.090091	0.900913	0.006601	0.066006	0.834907	0.417454
2CB1	1384.16	102.4	1281.76	17886.15	10	0.090091	0.900913	0.006456	0.064561	0.836352	0.418176
2CB2	1427.06	102.4	1324.66	17886.15	10	0.090091	0.900913	0.006672	0.066722	0.834191	0.417095
3CA1	2250.95	102.4	2148.55	26829.23	10	0.135137	1.35137	0.010822	0.108221	1.243149	0.621574
3CA2	2228.47	102.4	2126.07	26829.23	10	0.135137	1.35137	0.010709	0.107089	1.244281	0.622141
3CB1	2197.58	102.4	2095.18	26829.23	10	0.135137	1.35137	0.010553	0.105533	1.245837	0.622918
3CB2	2191.65	102.4	2089.25	26829.23	10	0.135137	1.35137	0.010523	0.105234	1.246136	0.623068
4CA1	3104.02	102.4	3001.62	35772.3	10	0.180183	1.801826	0.015119	0.15119	1.650637	0.825318
4CA2	3119.76	102.4	3017.36	35772.3	10	0.180183	1.801826	0.015198	0.151982	1.649844	0.824922
4CB1	3244.19	102.4	3141.79	35772.3	10	0.180183	1.801826	0.015825	0.15825	1.643577	0.821788
4CB2	3296.84	102.4	3194.44	35772.3	10	0.180183	1.801826	0.01609	0.160902	1.640925	0.820462
5CA1	4178.35	102.4	4075.95	44715.38	10	0.225228	2.252283	0.02053	0.205303	2.04698	1.02349
5CA2	4126.11	102.4	4023.71	44715.38	10	0.225228	2.252283	0.020267	0.202672	2.049611	1.024806
5CB1	4128.64	102.4	4026.24	44715.38	10	0.225228	2.252283	0.02028	0.202799	2.049484	1.024742
5CB2	4176.75	102.4	4074.35	44715.38	10	0.225228	2.252283	0.020522	0.205222	2.047061	1.02353

Day 1 Desorption	Radioactivity Readings disintegration per minute (dpm)				Volume	Original Conc	Original Mass	Conc. supernatant	Mass in supernatant	Mass adsorbed	Conc adsorbed
Sample	Supernatant (A)	V(mls)	Co (µg/ml)	(Mo) VCo(µg)	Cw	Mw CwV	Ms (Mo - Mw)	Cs (Ms/ms)	Mw CwV	Ms (Mo - Mw)	Cs (Ms/ms)
1CA1	449.82	234.35	215.47	17299.09	10	0.087134	0.425802	0.001085	0.010853	0.414949	0.207475
1CA2	**415.00**	234.35	180.65	17299.09	10	0.087134	0.425691	0.00091	0.009099	0.416591	0.208296
1CB1	390.92	234.35	156.57	17299.09	10	0.087134	0.422143	0.000789	0.007886	0.414257	0.207129
1CB2	402.10	234.35	167.75	17299.09	10	0.087134	0.425732	0.000845	0.008449	0.417283	0.208641
2CA1	774.30	234.35	539.95	17299.09	10	0.087134	0.834524	0.00272	0.027197	0.807327	0.403663
2CA2	768.35	234.35	534	17299.09	10	0.087134	0.834907	0.00269	0.026897	0.80801	0.404005
2CB1	735.33	234.35	500.98	17299.09	10	0.087134	0.836352	0.002523	0.025234	0.811118	0.405559
2CB2	770.41	234.35	536.06	17299.09	10	0.087134	0.834191	0.0027	0.027001	0.80719	0.403595
3CA1	1035.61	234.35	801.26	17299.09	10	0.087134	1.243149	0.004036	0.040359	1.20279	0.601395
3CA2	**1061.01**	234.35	826.66	17299.09	10	0.087134	1.244281	0.004164	0.041638	1.202643	0.601321
3CB1	1050.93	234.35	816.58	17299.09	10	0.087134	1.245837	0.004113	0.041131	1.204706	0.602353
3CB2	1061.29	234.35	826.94	17299.09	10	0.087134	1.246136	0.004165	0.041652	1.204483	0.602242
4CA1	1421.21	234.35	1186.86	17299.09	10	0.087134	1.650637	0.005978	0.059781	1.590855	0.795428
4CA2	1451.75	234.35	1217.4	17299.09	10	0.087134	1.649844	0.006132	0.06132	1.588524	0.794262
4CB1	1441.75	234.35	1207.4	17299.09	10	0.087134	1.643577	0.006082	0.060816	1.582761	0.79138
4CB2	1427.15	234.35	1192.8	17299.09	10	0.087134	1.640925	0.006008	0.060081	1.580844	0.790422
5CA1	1711.95	234.35	1477.6	17299.09	10	0.087134	2.046980	0.007443	0.074426	1.972554	0.986277
5CA2	1709.79	234.35	1475.44	17299.09	10	0.087134	2.049611	0.007432	0.074317	1.975295	0.987647
5CB1	1719.54	234.35	1485.19	17299.09	10	0.087134	2.049484	0.007481	0.074808	1.974676	0.987338
5CB2	1702.66	234.35	1468.31	17299.09	10	0.087134	2.047060	0.007396	0.073958	1.973103	0.986551

Desorption Day 2	Radioactivity Readings disintegration per minute (dpm)				Volume	Original Conc	Original Mass	Conc. supernatant	Mass in supernatant	Mass adsorbed	Conc adsorbed
Sample	Supernatant (A)	V(mls)	Co (µg/ml)	(Mo) VCo(µg)	Cw	Mw CwV	Ms (Mo - Mw)	Cs (Ms/ms)	Mw CwV	Ms (Mo - Mw)	Cs (Ms/ms)
1CA1	331.11	86.69	244.42	15497.15	10	0.078058	0.414949	0.001231	0.012311	0.402638	0.201319
1CA2	431.10	86.69	344.41	15497.15	10	0.078058	0.416591	0.001735	0.017348	0.399244	0.199622
1CB1	327.49	86.69	240.80	15497.15	10	0.078058	0.414257	0.001213	0.012129	0.402128	0.201064
1CB2	529.54	86.69	442.85	15497.15	10	0.078058	0.417283	0.002231	0.022306	0.394977	0.197488
2CA1	839.40	86.69	752.71	15497.15	10	0.078058	0.807327	0.003791	0.037913	0.769413	0.384707
2CA2	578.18	86.69	491.49	15497.15	10	0.078058	0.808010	0.002476	0.024756	0.783254	0.391627
2CB1	581.35	86.69	494.66	15497.15	10	0.078058	0.811118	0.002492	0.024916	0.786202	0.393101
2CB2	562.40	86.69	475.71	15497.15	10	0.078058	0.807190	0.002396	0.023961	0.783229	0.391614
3CA1	780.61	86.69	693.92	15497.15	10	0.078058	1.202790	0.003495	0.034952	1.167838	0.583919
3CA2	762.24	86.69	675.55	15497.15	10	0.078058	1.202643	0.003403	0.034027	1.168616	0.584308
3CB1	781.29	86.69	694.60	15497.15	10	0.078058	1.204706	0.003499	0.034987	1.16972	0.58486
3CB2	820.20	86.69	733.51	15497.15	10	0.078058	1.204483	0.003695	0.036946	1.167537	0.583768
4CA1	1003.74	86.69	917.05	15497.15	10	0.078058	1.590855	0.004619	0.046191	1.544664	0.772332
4CA2	992.18	86.69	905.49	15497.15	10	0.078058	1.588524	0.004561	0.045609	1.542915	0.771458
4CB1	1022.18	86.69	935.49	15497.15	10	0.078058	1.582761	0.004712	0.04712	1.535641	0.76782
4CB2	1045.42	86.69	958.73	15497.15	10	0.078058	1.580844	0.004829	0.048291	1.532553	0.766277
5CA1	1223.66	86.69	1136.97	15497.15	10	0.078058	1.972554	0.005727	0.057268	1.915286	0.957643
5CA2	1201.09	86.69	1114.40	15497.15	10	0.078058	1.975295	0.005613	0.056132	1.919163	0.959581
5CB1	1218.55	86.69	1131.86	15497.15	10	0.078058	1.974676	0.005701	0.057011	1.917665	0.958832
5CB2	1181.67	86.69	1094.98	15497.15	10	0.078058	1.973103	0.005515	0.055153	1.91795	0.958975

Desorption Day 3	Radioactivity Readings disintegration per minute (dpm)				Volume	Original Conc	Original Mass	Conc. supernatant	Mass in supernatant	Mass adsorbed	Conc adsorbed
Sample	Supernatant (A)	V(mls)	Co (µg/ml)	(Mo) VCo(µg)	Cw	Mw CwV	Ms (Mo - Mw)	Cs (Ms/ms)	Mw CwV	Ms (Mo - Mw)	Cs (Ms/ms)
1CA1	353.72	81.37	272.35	14544.95	10	0.073262	0.402638	0.001372	0.013718	0.38892	0.19446
1CA2	303.17	81.37	221.80	14544.95	10	0.073262	0.399244	0.001117	0.011172	0.388072	0.194036
1CB1	273.59	81.37	192.22	14544.95	10	0.073262	0.402128	0.000968	0.009682	0.392446	0.196223
1CB2	405.77	81.37	324.40	14544.95	10	0.073262	0.394977	0.001634	0.01634	0.378637	0.189318
2CA1	511.96	81.37	430.59	14544.95	10	0.073262	0.769413	0.002169	0.021689	0.747725	0.373862
2CA2	502.54	81.37	421.17	14544.95	10	0.073262	0.783254	0.002121	0.021214	0.76204	0.38102
2CB1	479.19	81.37	397.82	14544.95	10	0.073262	0.786202	0.002004	0.020038	0.766164	0.383082
2CB2	475.14	81.37	393.77	14544.95	10	0.073262	0.783229	0.001983	0.019834	0.763395	0.381697
3CA1	665.9	81.37	584.53	14544.95	10	0.073262	1.167838	0.002944	0.029442	1.138395	0.569198
3CA2	647.07	81.37	565.70	14544.95	10	0.073262	1.168616	0.002849	0.028494	1.140122	0.570061
3CB1	619.12	81.37	537.75	14544.95	10	0.073262	1.16972	0.002709	0.027086	1.142634	0.571317
3CB2	640.47	81.37	559.10	14544.95	10	0.073262	1.167537	0.002816	0.028161	1.139375	0.569688
4CA1	831.7	81.37	750.33	14544.95	10	0.073262	1.544664	0.003779	0.037794	1.506871	0.753435
4CA2	819.55	81.37	738.18	14544.95	10	0.073262	1.542915	0.003718	0.037182	1.505734	0.752867
4CB1	843.04	81.37	761.67	14544.95	10	0.073262	1.535641	0.003836	0.038365	1.497276	0.748638
4CB2	845.58	81.37	764.21	14544.95	10	0.073262	1.532553	0.003849	0.038493	1.494061	0.74703
5CA1	1001.24	81.37	919.87	14544.95	10	0.073262	1.915286	0.004633	0.046333	1.868953	0.934476
5CA2	989.41	81.37	908.04	14544.95	10	0.073262	1.919163	0.004574	0.045737	1.873426	0.936713
5CB1	1029	81.37	947.63	14544.95	10	0.073262	1.917665	0.004773	0.047731	1.869933	0.934967
5CB2	1037.42	81.37	956.05	14544.95	10	0.073262	1.91795	0.004816	0.048156	1.869794	0.934897